Egypt. J. Chem. **Vol. 67**, No. 8. pp. 47 - 55 (2024)

Egyptian Journal of Chemistry

http://ejchem.journals.ekb.eg/

Pinuspalustrols A & B, Two Rare Dimeric Abietane-O-O-Abietane-Type Diterpenoids of Natural Colophony from *Pinuspalustris*

Mohamed H. Abd El-Razek,[a*] Ahmed A.F. Soliman,[b] Mohamed Aboelmagd,[b] Ahmed H. El-Desoky[b]

[a]*Chemistry of Natural Compounds Department, Institute of Pharmaceutical and Drug Industries Research, National Research Centre (NRC), 33 El-Behouth St., Dokki, Giza, P.O. 12622, Egypt*

[b]*Department of Pharmacognosy, Institute of Pharmaceutical and Drug Industries Research, National Research Centre (NRC), 33 El-Behouth St., Dokki, Giza, P.O. 12622, Egypt*

Abstract

Pinuspalustris' natural colophony produced two novel secondary metabolites, pinuspalustrols A (**1**) & B (**2**), a unique pair of C-7 epimeric dimers based on abietane-type diterpenoids linked *via* C7-C12' peroxyconjunction system. Additionally, their biogenesis-related diterpenoid monomers were previously reported (**3**-**10**). Spectroscopic techniques, particularly 1D and 2D NMR together with HREIMS, were used to elucidate theirplanar structures, while their relative configurations were decided by NOESY spectra, together with comparison with NMR data of known analouges. Both pinuspalustrols A (**1**) and B (**2**) possess a skeleton of 12-Hydroxyabieta-8,11,13-trien-7-yl 6α-Hydroxy-7-oxoabieta-8,11,13-trien-12-yl peroxide, but they are epimeric at position 7. It is noteworthy that chemical compounds **3**-**10** were first isolated from *P.palustris*.

Keywords: Colophony; *Pinus palustris*; Pinaceae; dimeric abietane; diterpenoid

1. Introduction

The structural variety of natural chemical compounds obtained from plants is linked to a range of biological activities, making them an invaluable resource for pharmacological studies and the creation of health-related products. Geranylgeranyl pyrophosphate (GGPP) is the source of diterpenoids, which are a vast class of structurally diverse terpenoids with different scaffolds that include acyclic, mono-, bi-, tri-, and tetracyclic carbon skeletons[1]. Diterpenoid dimers, a rare subclass of diterpenoids, consist of two 20-carbon diterpenoid units connected by ether, C–C, ester, or ring moiety bonds [2]. Within recent decades, there has been an increasing interest in study on naturally occurring diterpenoid dimers as a result of their structural complexity and diverse bioactivities [3-5].

Diterpenoid dimers are more difficult to determine structurally because they have more chiral centers and more complicated ring structures than their monomeric counterparts [6,7]. On top of that, it is now feasible to detect molecules at trace levels due to the advancement of purification and structure elucidation techniques, particularly preparative HPLC and sensitive high field NMR. The separation of stereoisomers, particularly those with intricate structures like diterpenoid dimers, was significantly sped up using chiral HPLC [2-5].

The families Pinaceae, Cupressaceae, Cephalotaxaceae, Podocarpaceae, and Taxaceae are

*Corresponding author e-mail: abdelrazek3@yahoo.com.
Received date 02 January 2024; revised date 01 February 2024; accepted date 06 February 2024
DOI: 10.21608/EJCHEM.2024.260239.9134

mostly part of the conifers, which are the biggest group of extant gymnosperms (officially the Division Coniferopsida) [8]. The Pinaceae family has medicinal and ecological significance. It is a member of one of the top 20 wealthy drug-producing families, which produced a significant number of official medications [9]. About 230 species are found in 10 genera within this family (e.g. *Pinus*, *Cathaya*, *Abies*, *Pseudolarix*&*Larix*) [10]. With approximately 110 species, 41 of which are endemic to People's Republic of China, and 12 of which are variations, *Pinus* is the biggest genus in the Pinaceae family [11]. An abundant quantity of oleoresin, which is mostly composed of mono-terpene, sesquiterpene, or diterpeneacids, is present in several coniferous species of the pine family (Pinaceae). [12]. Numerous *Pinus* species components and extracts have antibacterial, antimicrobial, anti-inflammatory, and antioxidant properties [13,14].

Figure 1. *Pinuspalustris* Mill. produced colophony rosin. https://thepharmacognosy.com/resins/

Colophony, a resin derived from *P. palustris* Mill., (Figure **1**) contains between 50 and 70 percent resin acids [15,16]. Oleoresins, or viscous solutions of mono- and diterpenoid chemicals, are released by *P. palustris* trees. Colophony is produced when the resins' volatile monoterpene portions evaporate [15,16]. Pine colophony is mostly composed of monoterpenes and diterpene acids [17]. Numerous industries, including the chemical, pharmaceutical, and cosmetic ones, employ colophony in their products [17]. Additionally, colophony is utilized in coatings, adhesive formulations, antifouling paints, and dry toners [17,18]. It has several uses, such as a sizing agent in papermaking, a modifier and an anti-corrosive for plastics, and a size for rubber or paper. Compounds of polyoxyphenylene-based polymers including rosin esters show good molding, melt fluidity, and thermal characteristics [17]. There have been reports on the detection of diterpenes in canvas painting varnishes and the characterization of natural resins from various sources [19,20].

This article further identified eight known abietane-type diterpenoids (**3**-**10**) and described the isolation and structural elucidation of two novel epimersof dimericabietanoid peroxides diterpenoids (**1**&**2**).

2. Materials and Methods

2.1. Reagents and apparatus

Digital polarimeter JASCO DIP-180 was used to detect optical rotations. Utilizing a Shimadzu UV-2401PC spectrometer, UV spectra were collected. The Perkin-Elmer 983 G spectrophotometer was used to collect IR spectra. On a Varian-Unity-Plus-400 spectrometer, 400 MHz for ^{1}H and 100 MHz for ^{13}C NMR spectra were acquired in $CDCl_3$ at room temperature using residual solvent signals as an internal reference(δ_H 7.26 ppm; δ_C 77.1 ppm). The units of measurement for chemical shifts are δ values (ppm) and coupling constants (*J*) are Hz (hertz). A Jeol-JMS-HX300 mass spectrometer was used to perform the HR-EI-MS and EI-MS experiments. Silica gel (230-400 mesh; Merck & Co., Inc.) was used for column chromatography (CC), and Sephadex LH-20 (Amersham Pharmacia, Uppsala, Sweden), as well as pre-coated silica gel plates (60 F-254; Merck & Co., Inc.), were used for TLC analysis.Agilant 1260 system was utilized for semi-preparative HPLC, employing a normal phase column (Purospher STAR Si, 5 µm, 250 × 10 mm; Merck & Co., Inc.) and a reversed phase column (Hypersil Gold C18, 5 µm, 250 × 4.6 mm; Thermo Scientific).

2.2. Plant material

Harraz Medicinal Plant and Food Business Company (http://www.harrazherbs.com, Cairo, Egypt) provided the colophony resin (*P. palustris*) of south Atlantic region. The presence of *P. palustris*Mill., is shown by the brownish rock pine rosin (Colophony) in Figure **1**. The resin was ground into mesh 36 powder prior to being utilized for acetone extraction.

2.3. Extraction and isolation

At room temperature, 1.0 kg of colophony (resin) was powdered and allowed to percolate three times with 6.0 L of acetone over 48, 24, and 24 hours. Concentration was achieved by evaporating the filtrate in a vacuum to yield a gummy mass of acetone extract (96.0 g). The crude extract was subjected to liquid-liquid fractionation using solvents of successively increasing polarities, petroleum ether (3.0 L, to produce 16.1 g), CH_2Cl_2 (4.0 L, to yield 59.5 g), EtOAc (3.0 L, 13.8 g), and *n*-BuOH (3.0 L, to give6.0 g).CH_2Cl_2 fraction was chromatographed on a silica gel column (1.0 kg, 100-200 mesh, 10 × 70 cm) eluted with a step gradient of CH_2Cl_2/MeOH (100:0, 50:1, 20:1, 10:1, 5:1, 2:1, 1:1) to yield 7 fractions A-G.Fr. A (100:0, 15.5 g) was separated into seven fractions (A1-A7) using petroleumether-$CHCl_3$-EtOAc gradient solutions (50:1:1, 20:1:1, 10:1:1, and 5:1:1) using a silica gel column (220.0 g, 200-300 mesh, 6 × 60 cm). Sub-fraction A7 (11.1 g) was further purified using hexane/EtOAc (19:1), yielding **3** (150.3 mg,t_R 46.1 min) and **4**(214.7 mg, t_R 52.3 min) after HPLC analysis. Fr. B (5.2 g) was chromatographed using mixes of PE/EtOAc (20:1, 10:1, 5:1, 2:1, 1:1, EtOAc) as eluents in a stepwise gradient mode on a silica gel column (320.0 g, 200–300 mesh, 6 × 60 cm). The former step yielded five sub-fractions (FrB1–FrB5). Compounds **5**(75.1 mg,t_R52.3 min) and **6**(150.3 mg,t_R59.9 min) were obtained by combining the sub-fractions (FrB3-FrB5) (1.5 g) and chromatographing them using Sephadex LH-20 (4.0 × 1500 cm, CH_2Cl_2/MeOH, 1:1). This was followed by preparative HPLC (CH_3CN/H_2O, 45:55, 8 mL/min). Combining fractions C, D, and E (13.8 g) yielded 9 fractions (FrCDE 1 - FrCDE 9) when they were chromatographed on a silica gel column (320.0 g, 200–300 mesh, 6 × 60 cm) using PE/EtOAc combinations (20:1, 10:1, 5:1, 2:1, 1:1, EtOAc) as eluents in a stepwise gradient process. FrCDE3-FrCDE7 were mixed (1.7 g) and chromatographed on Sephadex LH-20 (4.0 × 1500 cm, CH_2Cl_2/MeOH, 1:1). Compounds **7** (70.3 mg, t_R 55.0 min), **8** (47.9 mg, t_R 33.3 min)and **9** (45.9 mg, t_R 22.5 min) were obtained by preparative HPLC (CH_3CN/H_2O, 65:35, 8 mL/min). The same protocols were followed to produce six fractions (FrFG1–FrFG–6) by subjecting the combination of fractions F & G (4.5 g) to silica gel column (100.0 g, 200-300 mesh, 4.5 × 40 cm) chromatography eluted with PE/EtOAc (15:1, 10:1, 5:1, 2:1, 1:1, EtOAc). FrFG2-FrFG5 (1.3 g) sub-fractions were chromatographed on Sephadex LH-20 (4.0 × 1500 cm, CH_2Cl_2/MeOH, 1:1), and compounds**10** (12.6 mg, t_R 20.3 min), **1** (6.5 mg, t_R 29.1 min) and **2** (4.5 mg, t_R 31.1 min) were obtained by preparative HPLC (MeOH/H_2O, 55:45, 8 mL/min).

2.3.1. Pinuspalustrol A: 12-Hydroxyabieta-8,11,13-trien-7α-yl 6α-Hydroxy-7-oxoabieta-8,11,13-trien-12-yl peroxide (**1**); yellow oil;$[\alpha]_D^{25}$-21.4 (*c* = 0.50, $CHCl_3$); UV (MeOH) λ_{max} (log ε) 220 (3.42), 279 (3.26) nm; IR (KBr) ν_{max}3429, 2925, 2555, 1719, 1545, 1457, 1414, 1369, 1225, 1169, 990, 731 cm^{-1}; ^1H and ^{13}C NMR data, see Table **1**; EI-MS (%) *m/z* 616 (was not seen) [M]+, 316 (55) $[C_{20}H_{28}O_2]^+$, 300 (90) $[C_{20}H_{28}O_2]^+$,285 (64), 272 (75), 257 (55), 229 (88), 203 (100), 189 (50); HR-ESI-MS*m/z* 639.4018 $[M + Na]^+$(calcd 639.4020; $C_{40}H_{56}O_5Na^+$).

2.3.2. Pinuspalustrol B: 12-Hydroxyabieta-8,11,13-trien-7β-yl 6α-Hydroxy-7-oxoabieta-8,11,13-trien-12-yl peroxide (**2**); Gum; $[\alpha]_D^{25}$-11.5 (*c* = 0.61, $CHCl_3$); UV (MeOH) λ_{max} (log ε) 220 (3.42), 279 (3.26) nm; IR (KBr) ν_{max} 3429, 2925, 2555, 1719, 1545, 1457, 1414, 1369, 1225, 1169, 990, 731 cm^{-1}; ^1H and ^{13}C NMR data, see Table **1**; EI-MS (%) *m/z* 616 (was not seen) [M]+, 316 (55) $[C_{20}H_{28}O_2]^+$, 300 (90) $[C_{20}H_{28}O_2]^+$,285 (64), 272 (75), 257 (55), 229 (88), 203 (100), 189 (50); HR-ESI-MS *m/z* 639.4018$[M + Na]^+$(calcd 639.4020; $C_{40}H_{56}O_5Na^+$).

3. Results and discussion

After being suspended in water, the colophony (rosin) CH_3COCH_3 extract was successively fractionated using petroleum ether, CH_2Cl_2, EtOAc, and *n*-BuOH. The combined CH_2Cl_2-soluble fraction was purified using recurrent silica gel, Sephadex LH-20 column chromatography, together with normal and reversed phase semipreparative HPLC. In conjunction with eight knownabietane-type diterpenoids, abietic acid (**3**)[21], pimaric acid (**4**)[22], sugiol (**5**) [23], 6,7-dehydroferruginol (**6**)[24], 6-Hydroxy-5,6-dehydrosugiol (**7**)[25], 5,6-dehydrosugiol (**8**) [26], ferruginol (**9**) [27], 6□-hydroxysugiol (**10**) [28], two new epimersof dimericabietane-type diterpenoids, pinuspalustrol A: 12-Hydroxyabieta-8,11,13-trien-7α-yl 6α-Hydroxy-7-oxoabieta-8,11,13-trien-12-yl peroxide (**1**) and Pinuspalustrol B: 12-Hydroxyabieta-8,11,13-trien7βyl 6α-Hydroxy-7-oxoabieta-8,11,13-trien-12-yl peroxide (**2**) were obtained, (Figure **2**).

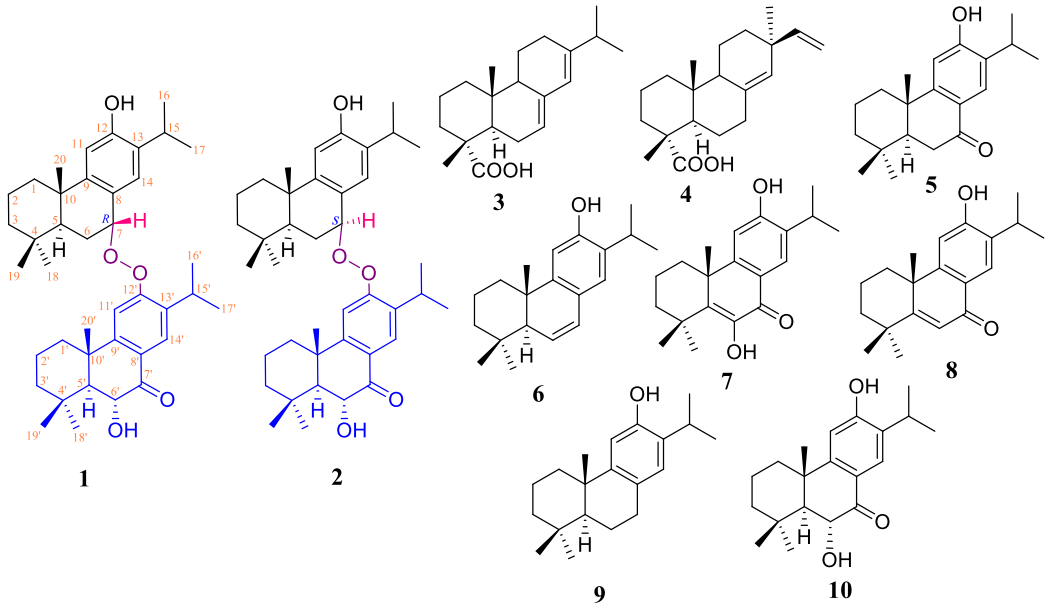

Figure 2.Chemical structures of compounds **1-10,** that were separated from *P. palustris*.

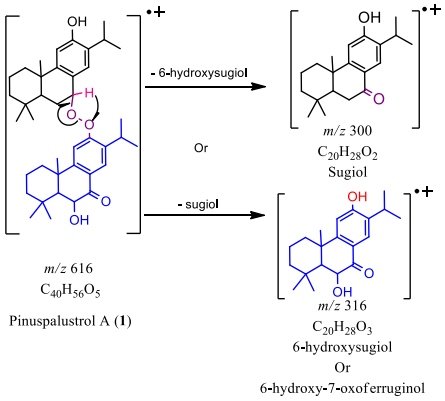

Figure **3**. A few significant EI-Mass fragmentations of **1**.

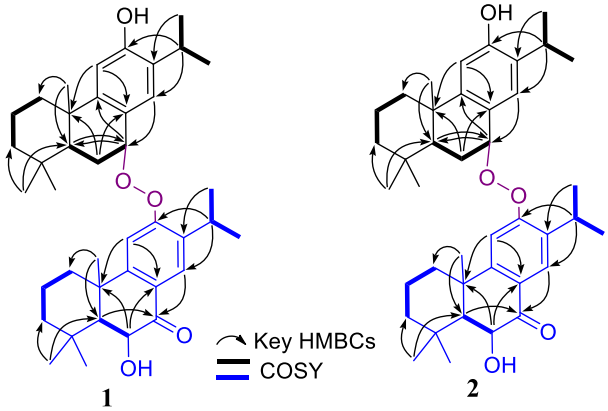

Figure **4**. Key HMBCs and COSY of **1** & **2**

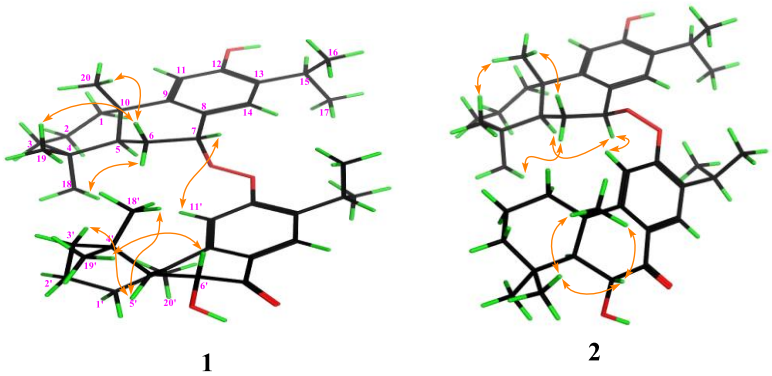

Figure **5**. Selective NOE correlations of **1** & **2**

Table **1**.Presents ^{1}H NMR data regarding compounds **1** and **2**.($CDCl_3$, 400 MHz for ^{1}H NMR, 100 MHz for ^{13}C NMR, δ in ppm, *J* in Hz).

	1		**2**			**1**		**2**	
No	δ_H	δ_C	δ_H	δ_C	No	δ_H	δ_C	δ_H	δ_C
1_{axi}	1.80 m	41.1	1.78 td (12.5, 2.7)	41.1	$1'_{axi}$	1.49 m	39.0	1.58 m	39.1
1_{eq}	1.95 br d (12.3)		1.96 br d (12.3)		$1'_{eq}$	2.39 m		2.28 br d (12.5)	
2	1.58 m	18.7	1.64 m	18.8	2'	1.77 m	18.9	1.68 m	18.8
3_{axi}	1.30 td (13.0, 3.5)	42.9	1.30 m	42.2	$3'_{axi}$	1.23 m	42.2	1.26 m	42.9
3_{eq}	1.50 m		1.50 m		$3'_{eq}$	1.51m		1.50 m	
4		34.6		34.7	4'		34.2		34.2
5	1.91 dd (12.2, 2.3)	43.5	1.72 dd (8.7, 3.2)	47.3	5'	1.81 d (10.0)	56.0	1.91 d (12.9)	56.2
6_{axi}	2.33 td (13.5, 12.2, 2.3)	33.8	2.40 dddd (13.5, 12.2, 2.3, 2.1)	34.7	6'	4.67 d (10.3)	73.9	4.64 d (10.3)	73.9
6_{eq}	2.23 dt (13.5, 2.3)		2.22 dt (13.5, 2.3)						
7	6.00 br t (3.1)	96.4	5.41 dd (9.2, 2.7)	102.3	7'		199.9		199.9
8		144.9		146.0	8'		121.7		123.3
9		142.3		142.6	9'		156.0		156.1
10		40.6		41.3	10'		39.6		39.7
11	6.71 s	113.4	6.76 s	114.1	11'	7.17 s	108.1	7.05 s	108.5
12		148.8		149.4	12'		158.9		159.7
13		132.0		133.1	13'		135.7		136.9
14	6.24 s	121.2	6.66 s	120.9	14'	7.78 s	126.3	7.95 s	126.6
15	2.85 sept. (7.0)	26.1	3.00 sept. (7.0)	27.5	15'	2.79 sept. (7.0)	27.3	3.29 sept. (7.0)	26.9
16	0.66 d (7.0)	22.5	1.13 d (7.0)	21.9	16'	0.74 d (7.0)	21.9	1.17 d (7.0)	22.5
17	0.97 d (7.0)	22.2	1.22 d (7.0)	21.9	17'	1.03 d (7.0)	22.2	1.22 s	22.6
18	0.99 s	33.5	1.22 s	35.8	18'	1.18 s	35.8	0.97 s	33.5
19	1.00 s	23.2	1.22 s	22.4	19'	1.24 s	21.9	1.02 s	23.2
20	1.36 s	21.5	1.46 s	21.9	20'	1.52 s	24.9	1.34 s	24.6
12-OH	3.91 s								

Pinuspalustrol A, a dimericditerpenoid**1**, was produced as an optically active $[\alpha]_D^{25}$-21.4 (*c* = 0.5, $CHCl_3$) with yellow oil. From the HRESIMS [M + Na]$^+$ ion at *m/z* 639.4015 (calcd 639.4020; $C_{40}H_{56}O_5Na^+$), its chemical formula was inferred to be $C_{40}H_{56}O_5$, which corresponds to thirteen indices of hydrogen insufficiency (IHDs). EIMS of **1**exhibitedfragment ions at *m/z* 300 $[C_{20}H_{28}O_2]^+$and 316 $[C_{20}H_{28}O_3]^+$ (Figure **3**), and the ^{13}C-NMR spectrum had forty carbon signals, indicating that **1** was a dimericditerpenoid and that its component monomers-1 $[C_{20}H_{28}O_2]$and -2 $[C_{20}H_{28}O_3]$, made up compound **1**. Its ultraviolet (UV) and infrared (IR) spectra further revealed the absorptions for the

following groups: hydroxyl (3429 cm^{-1}), benzoyl(1719 cm^{-1}; λ_{max} 220, and 279 nm), and aromatic (2925, 1545, and 1457 cm^{-1}).

Forty carbon signals have been detected in the ^{13}C NMR (Table **1**) which were supported by the aid of DEPT and HSQC spectra, which belong to ten methyls, seven methylenes, ten methines (four sp^3; four sp^2; two sp^3 oxygenated), and thirteen nonprotonated carbons [which include one carbonyl group δ_C 199.9 (C-7`); four sp3 quaternary δ_C 34.6 (C-4), 34.2 (C-4'), 40.6 (C-10), 39.6 (C-10'), and eight sp^2 carbons δ_C 144.9 (C-8), 142.3 (C-9), 148.8 (C-12), 132.0 (C-13), 121.7 (C-8'), 156.0 (C-9'), 158.9 (C-12'), 135.7 (C-13')]. Careful analysis of NMR data including COSY, HMQC and HMBC revealed that thirteen carbons and twenty seven carbon-bearing protons were represented by ten methylsin the high-filed, indicating
the diterpenoid characteristics classified as: a pairs of angular methyl [δ_H 1.36 (3H, s, Me-20)/δ_C 21.5 (Me-20), δ_H 1.52 (3H, s, Me-20')/δ_C 21.5 (Me-20')]; two pairs of germinal methyl [δ_H 0.99 (3H, s, Me-18)/δ_C 33.5 (Me-18), δ_H 1.00 (3H, s, Me-19)/δ_C 23.5 (Me-19), δ_H 1.18 (3H, s, Me-18')/δ_C 35.8 (Me-18'), δ_H 1.24 (3H, s, Me-19')/δ_C 21.9 (Me-19')] and two isopropyl groups attached to a phenyl groups [δ_H 0.66 (3H, d, *J* = 7.0 Hz, Me-16)/δ_C22.5 (Me-16), δ_H 0.97 (3H, d, *J* = 7.0 Hz, Me-17)/δ_C 22.2 (Me-17), δ_H 0.74 (3H, d, *J* = 7.0 Hz, Me-16')/δ_C 21.9 (Me-16'), δ_H 1.03 (3H, d, *J* = 7.0 Hz, Me-17')/δ_C 22.2 (Me-17')], four *para* aromatic protons [δ_H 6.71 (1H, s, H-11)/δ_C 113.4 (C-11), δ_H 6.24 (1H, s, H-14)/δ_C 121.2 (C-14), δ_H 7.17 (1H, s, H-11')/δ_C 108.1 (C-11'), δ_H 7.78 (1H, s, H-14')/δ_C 126.3 (C-14')], four aliphatic prontons [δ_H 1.91 (1H, dd, *J* = 12.2, 2.3 Hz, H-5)/δ_C 43.5 (C-5), δ_H 2.85 (1H, sept, *J* = 7.0 Hz, H-15)/δ_C 26.1 (C-15), δ_H 1.81 (1H, d, *J* = 10.0 Hz, H-5')/δ_C 56.0 (C-5'), δ_H 2.79 (1H, sept, *J* = 7.0 Hz, H-15')/δ_C 27.3 (C-15')], seven methylenes [from δ_H 1.30 ≈ 2.39/δ_C 41.1 (C-1), 39.0 (C-1'), 18.7 (C-2), 18.9 (C-2'), 42.9 (C-3), 42.2 (C-3') and the most one downfield at δ_H 2.33 (1H, td, *J* = 13.5, 12.2, 2.3 Hz, H-6_{axi}), 2.23 (1H, dt, *J* = 13.5, 2.3 Hz, H-6_{eq})/δ_C 33.8 (C-6)], and two oxymethines [δ_H 6.00 (1H, br t, *J* = 3.1 Hz, H-7)/δ_C 96.4 (C-7), δ_H 4.67 (1H, d, *J* = 10.3 Hz, H-6')/δ_C 73.9 (C-6')], besidesa phenolic hydroxyl proton δ_H 3.91 (1H, s, exchangeable with D_2O) (Table **1**). Four unique quaternary signals at δ_C 34.6 (C-4), 40.6 (C-10), 34.2 (C-4'), and 39.6 (C-10') were revealed by the ^{13}C and DEPT NMR spectroscopy data, together with a distinctive downshifted Hβ-1 signal δ_H 1.95 (1H, br d, *J* = 12.3 Hz) supported the hypothesis for abietanediterpenoid core skeleton of **1**. These data suggested that compound **1** ought to consist of two abietanediterpenoids dimers [29-31]. The aforementioned NMR results displayed that the molecule's constituent monomer-1 (half of the molecule) is linked to 7-hydroxyferruginol while its constituent monomer-2 (half of the molecule) is linked to 6-hydroxy-7-oxoferruginol [32].

The planner structure of (monomer-1) of **1** was developed along with proton spin systems H_2-1/H_2-2/H_2-3 and H-5/H-6/H-7 derived from the ^1H-^1H COSY spectrum (Fig. 3). In addition to, the HMBC correlations (Fig. 3) from Me-20/C-1, C-5, C-9 and C-10; from Me-18 & Me-19/C-3, C-4, C-5; from H-15/C-12, C-13, C-14; from H-14/C-7, C-9, C-12; and from H-7/C-5,C-8,C-9. The gross structure of (monomer-2) of **1** was elucidated from the HMBC correlations (Figure **4**) from Me-18'& Me-19'/C-3', C-4', C-5'; from H-15'/C-12', C-13', C-14'; from H-14'/C-7', C-9', C-12'; from H-5'/C-4', C-6', as well as two proton spin systems, H_2-1'/H_2-2'/H_2-3' and H-5'/H-6', observed from the ^1H-^1H COSY spectrum (Fig. 3). The NMR data of the monomer-1 exhibited a resemble features very similar to the monomer-2, except for the system of methylene protons (H_2-6) [δ_H 2.33 (1H, td, *J* = 13.5, 12.2, 2.3 Hz, H-6_{axi}), 2.23 (1H, dt, *J* = 13.5, 2.3 Hz, H-6_{eq})/δ_C 33.8 (C-6)] neighboring to a methine carbon bearing a peroxyl conjunction [δ_H 6.00 (1H, br t, *J* = 3.1 Hz, H-7)/δ_C 96.4 (C-7)] in monomer-1 was replaced by a methine carbon bearing a hydroxyl group [δ_H 4.67 (1H, d, *J* = 10.3 Hz, H-6')/δ_C 73.9 (C-6')] neighboring to a conjugated carbonyl (δ_C 199.9) system in the monomer-2. Launching with the monomer-2, comparing the other three singlet aromatics [δ_H 7.17 (H-11'), 6.71 (H-11) and 6.24 (H-14)], the singlet signal that appeared further downfield δ_H 7.78 (H-14'), was caused by the conjugated carbonyl (C-7') deshielding anisotropic effect. Following the assignment of the constitutional units, we focused on determining their connection to create the new dimer **1**'s gross structure. According to the chemical formula $C_{40}H_{56}O_5$, which was obtained by

HRESIMS, the molecule included two oxygen atoms that weren't connected to the rings core skeleton of the diterpenoiddimeric skeleton. As was previously mentioned, one of them was caused by the phenolic hydroxyl at position C-12 in HMBCs (Figure **4**). Two oxygenated carbon atoms were detected in the 13C NMR spectra; the first one was linked to the carbinol at δ_C 73.9, and the second one to the conjugated carbonyl at δ_C199.9 ppm. The two oxygen atoms left were in the form of peroxide, which joins C-7 and C-12' in order to generate the dimer **1**. Furthermore, a peroxide structure is compatible with the base peak at m/z 300 from the mass fragmentation pattern of **1**. On the basis of these data, the acceptance of the peroxide conjunction could be explained by the H-7 lower field signal [δ_H 6.00 (1H, br t, *J* = 3.1 Hz)], and δ_C 96.4 accord with the adverse effects upon one peroxide. Assigning H-7, we found that a downshifted benzyl proton connected to a peroxyl group [δ_H 6.00 (1H, br t, *J* = 3.1 Hz)] rather than a hydroxyl group [32,33] showed the ^{1}H-^{1}H COSY correlations to the two methylene protons of H-6 [δ_H 2.23 (1H, dt, *J* =13.5, 2.3 Hz, H-6$_{eq}$), δ_H 2.33 (1H, td, *J* =13.5, 12.2, 2.3 Hz, H-6$_{axi}$)] and HMBC correlations with C-5 (δC 43.5), C-8 (δC 144.9) and C-9 (δ_C 142.3). Furthermore, the proton signal of H-7 had NOESY correlations to both H-6$_{eq}$ and H-6$_{axi}$ and was a broad triplet peak with a tiny coupling constant, *J* = 3.1 Hz. This would indicate that the peroxyl group was bonded on C-7 in α-*axial* orientation. Compound 1's spatial conformation is really fascinating. Since the benzoyl group of the lower unit (monomer-2) 6α-hydroxy-7-oxoferruginol derivative is an electron-poor site, the phenol functionality of the higher (monomer-1) 7α-peroxyferruginol derivative is an electron-rich site. Based on their mutual attraction, the two aromatic features will form the most stable conformer, as Figure **5** exhibits. Due to the opposing phenyl group's anisotropic impact, the chemical shifts of H-14', H-15', H-16', H-17', H-14, H-15, H-16, and H-17 upshifted to the high field region. However, H-5, H-7, and H-20' of 1 were positioned in the deshielding region, indicating that their field chemical shifts are lower than those of the typical dehydroabietanediterpene[34]. Concurrently, a NOESY association correlation (Figure **5**) was discovered between H-7 and H-11′ confirming the connection of both monomers.Meanwhile, H$_3$-19'/H-6' NOE confirmed the *β*-configuration of H-6'. On the other hand, the biosynthetic similarity of both the northern monomer with sugiol and the southern monomer with 6-hydroxusugiol suggests the relative configuration of **1** as shown in figure 2. With the use of the DEPT, ^{1}H-^{1}H COSY, NOESY, HMQC, and HMBC, clear full assignments for the ^{1}H and ^{13}C NMR signals in the dimer **1** were made. Based on the magnitude of the coupling constant, which corresponds to the vicinal spin-spin interaction with NOE correlations, the relative stereochemistry of H-7 was conjectured, and as a result, the relative configuration at C-7 should be *R**. Compound **1** was therefore identified as 12-Hydroxyabieta-8,11,13-trien-7α-yl 6α-Hydroxy-7-oxoabieta-8,11,13-trien-12-yl peroxide and was given a trivial name pinuspalustrol A.

Based on HRESIMS data, pinuspalustrol B (**2**) was produced as pale yellowish oil with the same chemical formula ($C_{40}H_{56}O_5$) as **1**. The structure of **2** appeared to be a typical similarity with **1** believed to be analogues, according to the EIMS, UV, and IR data.In the ^{13}C NMR (^{1}H and DEPT) spectra of **2**, 56 signals corresponding to 40 carbon atoms were also utilized to categorize the molecule as a diterpenoid dimer type, equivalent with two monmers moieties that each contained 20 carbon atoms (Table **1**). These findings are compatible with supporting the concept for an abietanediterpenoid dimer core skeleton of **2**, along with ^{1}HNMR (1D and 2D), HMQC, and HMBC spectra. The proposed planar structure of **2** (Table **1**) should be identical to **1** according to a detailed examination of the ^{1}H and ^{13}C NMR data. The NMR spectrum data of the dimeric structures **1** and **2** exhibit a considerable discrepancy, which is explained by these results, which indicated that the chiral carbons of **1** and **2** had the same configuration as depicted in their conformation, with the exception of the chiral C-7. By using HMBC (Figure **4**) and NOESY (Figure **5**) spectra, it was possible to clearly see the peroxy junction (C-7 & C-12') of the two abietane-type diterpenoid moieties in **2**. A powerful and visible $^4J_{CH}$ connection from H-7 to C-12' (δ_C 159.7) in the HMBC spectrum of **2** corroborated the existence of a proxy junction. A thorough analysis of **2** and **1**'s ^{1}H and ^{13}C NMR data showed quite variations in C-7, indicating they were probably stereoisomers. The HMBC determined the chemical shifts of the prochiralhydrogens H$_{R*}$-7 (**1**, δ_H 6.00) and H$_{S*}$-7 (**2**, δ_H 5.41), most likely as a result of their more favorable dihedral angles as observed in the

models in Fig. 4. The minimized structures of **1** and **2**demonstrate hydrogen's that obstruct the diastereotopic. The lowest energy conformation of **1** and **2** additionally enabled us to observe that H_{R*}-7 (**1**) is located in a deshielding region of the aromatic ring C's β-face, causing a shift to be more down field, whereas H_{S*}-7 (**2**) is located in a sheilding region of the ring C's α-face, causing a shift to be more up field [$\Delta\delta_H = 5.41_{HS*\text{-}7\ (2)} - 6.00_{HR*\text{-}7\ (1)} = -0.59$ ppm]. In light of the ^{13}C NMR spectroscopy's sensitivity for identifying conformational changes, a spectral comparison between compounds **1** and **2** revealed significant gaps in the chemical shifts of a C-7. The significant downfield shift including in the deshielding of the C-7 [$\Delta\delta_C$ = 102.3 (**2**) – 96.4 (**1**) = + 5.9 ppm] of **2** by +5.9 ppm is caused by the γ-gauche effect from various orientation of the peroxy junction at it. Based on the relevant proton's (H-7) coupling constant values, which showed values of 9.2 Hz for the vicinal *axial-axial* coupling with H-6_{axi} and 2.7 Hz for the vicinal *axial-equatorial* coupling with H-6_{eq}, it was confirmed that C-7 is in an *S**-configuration with respect to H-7, intended to be in an *axial* spatial orientation. As, compounds **1** and **2** exhibit different ^{13}C NMR chemical shifts, as well as the ^{1}H NMR and coupling constants reported for H-7 indicate an alternative configuration for the C-7 stereogenic center. The NOESY (Figure **5**) studies were conducted using compounds **1** and **2**, with the aim of verifying the relative stereochemistry illustrated for compound **2**. Therefore, although there was a noticeable NOE cross-peak in compound **2** between protons H-7 and H-5, there was not a cross-peak between these protons in the comparable NOESY spectra of compound **1**.Additionally, compound **2**'s proposed relative stereochemistry agreed with the cross-peaks between H-5 and H-7 for pro-*S** that were seen, as well as compound **1**'s total absence with pro-*R**.On the other hand, the *β*-configuration of H-6' was decided by H-7'/H_3-19' and H-7'/H_3-20' NOEs. Biosynthetic considerations suggested the relative configurations of **2** in a similar manner as for **1** (Fig. 2). Consequently, it was established that dimeric**2** was 7-*epi*-pinuspalustrol A (**1**).

4. Conclusions

Two unique epimersdimericabietanoid peroxides (**1**&**2**) were isolated in the present investigation through acetone extract with several chromatographic techniques during the phytochemical examination of the naturally occurring rosin colophony (*Pinuspalustris*). Additionally, eight known abietane-type diterpenoids were also identified (**3**-**10**).

5. Conflicts of interest

"There are no conflicts to declare".

6. Acknowledgments

Authors acknowledge National Research Centre for supporting research facilities.

7. References

1. Hanson JR, Nichols T, Mukhrish Y, et al. Diterpenoids of terrestrial origin. Natural Product Reports. 2019;36(11):1499-1512.
2. Cheng B, Chen Y-S, Pu X, et al. Callicarpnoids A–C, structurally intriguing ent-Clerodane diterpenoid dimers with cytotoxicity against MCF-7 and HCT-116 cell lines from Callicarpa arborea Roxb. Bioorganic Chemistry. 2022;129:106111.
3. Liu J, He X-F, Wang G-H, et al. Aphadilactones A–D, four diterpenoid dimers with DGAT inhibitory and antimalarial activities from a Meliaceae plant. The Journal of Organic Chemistry. 2014;79(2):599-607.
4. Zhang H-J, Zhang Y-M, Luo J-G, et al. Anti-inflammatory diterpene dimers from the root barks of Aphanamixis grandifolia. Organic & Biomolecular Chemistry. 2015;13(27):7452-7458.
5. Zhang H, Liu J, Gan L-S, et al. Antimalarial diterpenoid dimers of a new carbon skeleton from Aphanamixis grandifolia. Organic & Biomolecular Chemistry. 2016;14(3):957-962.
6. Peng Y, Chang Y, Sun C, et al. Octacyclic and decacyclic ent-abietane dimers with cytotoxic activity from Euphorbia fischeriana steud. Chinese Chemical Letters. 2022;33(9):4261-4263.
7. Vasas A, Hohmann J. Euphorbia diterpenes: isolation, structure, biological activity, and synthesis (2008–2012). Chemical reviews. 2014;114(17):8579-8612.
8. Xiong J, Hu C-L, Wang P-P, et al. Spirobiflavonoid stereoisomers from the endangered conifer Glyptostrobus pensilis and their protein tyrosine phosphatase 1B inhibitory activity. Bioorganic & Medicinal Chemistry Letters. 2020;30(4):126943.
9. Ibrahim MA, Na M, Oh J, et al. Significance of endangered and threatened plant natural products in the control of human disease. Proceedings of the National Academy of Sciences. 2013;110(42):16832-16837.
10. Zhu F, Qin C, Tao L, et al. Clustered patterns of species origins of nature-derived drugs and clues for future

bioprospecting. Proceedings of the National Academy of Sciences. 2011;108(31):12943-12948.
11. Hu C-L, Xiong J, Gao L-X, et al. Diterpenoids from the shed trunk barks of the endangered plant Pinus dabeshanensis and their PTP1B inhibitory effects. RSC advances. 2016;6(65):60467-60478.
12. Liu J, Li J-J, Yan Y-M, et al. COX-2 and iNOS inhibitory abietane diterpenoids from Pinus yunnanensis exudates. Fitoterapia. 2023;164:105376.
13. Grassmann J, Hippeli S, Vollmann R, et al. Antioxidative properties of the essential oil from Pinus mugo. Journal of agricultural and food chemistry. 2003;51(26):7576-7582.
14. Li B, Shen Y-H, He Y-R, et al. Chemical constituents and biological activities of Pinus species. Chemistry & biodiversity. 2013;10(12):2133-2160.
15. Berg KJvd, Boon JJ, Pastorova I, et al. Mass spectrometric methodology for the analysis of highly oxidized diterpenoid acids in Old Master paintings. Journal of mass spectrometry. 2000;35(4):512-533.
16. Van der Werf ID, van den Berg KJ, Schmitt S, et al. Molecular characterization of copaiba balsam as used in painting techniques and restoration procedures. Studies in Conservation. 2000;45(1):1-18.
17. Gören AC, Bilsel G, Öztürk AH, et al. Chemical composition of natural colophony from Pinus brutia and comparison with synthetic colophony. Natural Product Communications. 2010;5(11):1934578X1000501105.
18. Baytop T. Therapy with medicinal plants in Turkey. Past and Present. 1999;2:348-349.
19. Chiavari G, Fabbri D, Prati S. Characterisation of natural resins by pyrolysis—Silylation. Chromatographia. 2002;55:611-616.
20. Osete-Cortina L, Doménech-Carbó MT, Mateo-Castro R, et al. Identification of diterpenes in canvas painting varnishes by gas chromatography–mass spectrometry with combined derivatisation. Journal of Chromatography A. 2004;1024(1-2):187-194.
21. Kruk C, De Vries N, Van der Velden G. Two-dimensional INADEQUATE 13C NMR studies of maleopimaric acid, the diels–alder adduct of levopimaric acid and maleic anhydride, and of abietic acid. Magnetic resonance in chemistry. 1990;28(5):443-447.
22. Sahu B, Bhardwaj N, Chatterjee E, et al. LCMS-DNP based dereplication of Araucaria cunninghamii Mudie gum-resin: identification of new cytotoxic labdane diterpene. Natural Product Research. 2022;36(24):6207-6214.
23. Rodríguez B. 1H and 13C NMR spectral assignments of some natural abietane diterpenoids. Magnetic Resonance in Chemistry. 2003;41(9):741-746.
24. González AG, Aguiar ZE, Grillo TA, et al. Diterpenes and diterpene quinones from the roots of Salvia apiana. Phytochemistry. 1992;31(5):1691-1695.
25. Bazzocchi IL, Núñez MJ, Reyes CP. Bioactive diterpenoids from Celastraceae species. Phytochemistry Reviews. 2017;16:861-881.
26. Matsumoto T, Tanaka Y, Terao H, et al. The synthesis of salvinolone, saprorthoquinone, and 4-hydroxysapriparaquinone from (+)-dehydroabietic acid. Bulletin of the Chemical Society of Japan. 1993;66(10):3053-3057.
27. Jassbi AR, Hadavand Mirzaei H, Firuzi O, et al. Cytotoxic abietane-type diterpenoids from roots of Salvia spinosa and their in Silico pharmacophore modeling. Natural Product Research. 2022;36(12):3183-3188.
28. Naman CB, Gromovsky AD, Vela CM, et al. Antileishmanial and cytotoxic activity of some highly oxidized abietane diterpenoids from the bald cypress, Taxodium distichum. Journal of natural products. 2016;79(3):598-606.
29. Xiao Q-L, Xia F, Yang X-W, et al. New dimeric and seco-abietane diterpenoids from Salvia wardii. Natural Products and Bioprospecting. 2015;5:77-82.
30. Fraga BM, Diaz CE, López-Rodríguez M. Two novel abietane dimers from transformed root cultures of Salvia broussonetii. Tetrahedron Letters. 2014;55(4):877-879.
31. Xu J, Chang J, Zhao M, et al. Abietane diterpenoid dimers from the roots of Salvia prionitis. Phytochemistry. 2006;67(8):795-799.
32. Arihara S, Umeyama A, Bando S, et al. A new abietane and two dimeric abietane diterpenes from the black heartwood of Cryptomeria japonica. Chemical and pharmaceutical bulletin. 2004;52(3):354-358.
33. Dellar JE, Cole MD, Waterman PG. Antimicrobial abietane diterpenoids from Plectranthus elegans. Phytochemistry. 1996;41(3):735-738.
34. Seca AM, Silva AM, Bazzocchi IL, et al. Diterpene constituents of leaves from Juniperus brevifolia. Phytochemistry. 2008;69(2):498-505.